PHYSICAL REVIEW B VOLUME 37, NUMBER 14 15 MAY 1988-I

Size effects on the vacancy-formation energy of small sodium clusters in the jellium model

C. Baladrón
Departamento de Física Aplicada III, Universidad de Valladolid, Valladolid, Spain

J. A. Alonso and M. P. Iñiguez
Departamento de Física Teórica, Universidad de Valladolid, Valladolid, Spain

(Received 5 October 1987; revised manuscript received 8 December 1987)

The vacancy-formation energy ΔE_f in small sodium clusters (Na_N, $N < 94$) is calculated using the density-functional formalism. The clusters are simulated by a jellium background model. According to this model, strong oscillations are predicted for ΔE_f in the size range studied, which makes it difficult to advance any conclusions about the evolution of ΔE_f for larger values of N. The oscillations in ΔE_f can be explained by looking at the binding energy of perfect and defect clusters and in simple terms by looking at the shift of one-electron levels induced by the formation of the vacancy. ΔE_f has large values for the experimental "magic clusters." On the other hand, low values of ΔE_f correlate with clusters which become ellipsoidally deformed in Clemenger's ellipsoidal model.

I. INTRODUCTION

There is some theoretical discussion about the size dependence of the concentration of vacancies in highly dispersed systems[1,2] and about the effect that an increased vacancy concentration at high dispersion might have on a number of observed properties, like the change in the temperature of polymorphous transformations, the decrease in the lattice constant, the increase in the compressibility, or the increase in the solubility associated with a decrease in the particle size.[1] Morokhov, Zubov, and Fedorov[2] have shown that, in the case of metal particles, the vacancy-formation energy ΔE_f depends on the competition of effects of similar magnitude but opposite sign, which makes it very difficult to predict if ΔE_f differs with respect to the value for a bulk crystal.

Detailed microscopic calculations of ΔE_f as a function of size could then be of some potential interest if the size variation of the properties mentioned above (or others) is related to a possible enhanced concentration of vacancies. As a first attempt in this direction, we study the size variation of ΔE_f for vacancies formed in small sodium clusters, simulated by a jelliumlike model. The theoretical tool used is the density-functional formalism.[3] This method, combined with a spherical jellium model background, has been very successful in explaining the main features of the mass distribution of alkaline clusters formed in supersonic expansions,[4–7] and more specifically, the correspondence between the observed magic numbers (occurring for a number of atoms $N = 2$, 8, 20, 40, 58, and 92) and spherical clusters with filled electronic shells.

Our main result here is the prediction that ΔE_f oscillates strongly as the cluster size increases ($N \lesssim 100$), and that these oscillations are linked to the electronic shell filling effect that also governs the stability variations of perfect simple-metal clusters. The large oscillations of ΔE_f with size prevent us from drawing conclusions about a possible relation between the vacancy concentration and the kind of properties mentioned above for ultradispersed metals. One should deal with larger particles, where quantum effects are attenuated, to be able to draw such conclusions. Our results for very small particles ($N < 100$) are, however, interesting in themselves. In addition, it might be possible to extract from our calculations some useful implications about the interpretation of the mass distribution of compound clusters.[8]

II. MODEL CALCULATION

To obtain the vacancy-formation energy we have subtracted the total energy of the perfect cluster from that of the cluster with a vacancy at its center. The perfect cluster is characterized by the jellium model. Each sodium atom contributes one valence electron to an electron gas immersed in a neutralizing positive background with constant density n_0^+ and spherical shape. n_0^+ is taken the same as for bulk sodium and the cluster radius R evidently depends upon the number of atoms. The electron density $\rho(\mathbf{r})$ and the total energy of the cluster are self-consistently calculated by solving the Kohn-Sham equations of the density-functional theory, the local-density approximation being used for exchange and correlation (see Refs. 9 and 10 for details).

Then, a vacancy is introduced in the cluster by removing one atom from the cluster center and placing it at the surface. This is achieved within the jellium model by redistributing the positive background density such that

$$n^+(r) = \begin{cases} 0, & r < R_v \\ n_0^+, & R_v < r < R \\ 0, & R < r \end{cases} \tag{1}$$

where $R_v = 3.931$ a.u. is the radius of the "unrelaxed" vacancy (it corresponds to the Wigner-Seitz radius of bulk sodium). The constant n_0^+ has, evidently, the same value as for the perfect cluster. However, the cluster radius R is different from that of the perfect cluster and is fixed by the normalization condition of the positive background change.

In a previous paper on aluminum clusters using, however, a pseudopotential model, it was found that the relaxation of the neighbors around the vacancy is very small.[11] We have also studied the same question in the jellium model by smoothing out the sharp discontinuity of $n^+(r)$ at $r=R_v$. We have then considered a linear dependence of $n^+(r)$ on the radial distance, around $r=R_v$, allowing for the variation of the slope. The condition of charge normalization fixes the rest of the intervening parameters. Minimization of the total energy of the system, obtained as well by the self-consistent density-functional formalism, with respect to the slope, then gives the optimum relaxation. This one occurs for the background given in Eq. (1). This background thus leads to the most stable vacancy in our model. Of course, one could imagine other models for a relaxed background but the result obtained suggests that the relaxation around the vacancy will be very small, in agreement with our earlier finding.[11]

III. RESULTS

The vacancy-formation energy $\Delta E_f(N)$ for a sodium cluster with N atoms is defined by

$$\Delta E_f(N)=E(N_v)-E(N) , \tag{2}$$

where $E(N)$ and $E(N_v)$ represent the total energies of the perfect cluster and the cluster with a vacancy at its center, respectively. The calculated vacancy-formation energy is plotted as a function of cluster size in Fig. 1. $\Delta E_f(N)$ shows pronounced oscillations as a function of cluster size. In the size range studied, $\Delta E_f(N)$ presents alternatively a maximum or a minimum for N corresponding to perfect clusters with filled electronic shells. Closing shell numbers for perfect jellium clusters are $N=2(1s)$, $8(1p)$, $18(1d)$, $20(2s)$, $34(1f)$, $40(2p)$, $58(1g)$, $68(2d)$, $90(1h)$, and $92(3s)$, which correspond to the successive filling of the cluster electronic shells given in brackets. Then we find maxima in ΔE_f for $N=8$, 20, 40, (66), and 92, and minima for $N=18$, 34, 58, and 90. Notice that the maximum at $N=66$, instead of 68, is the only exception to this rule. The reason will be explained later.

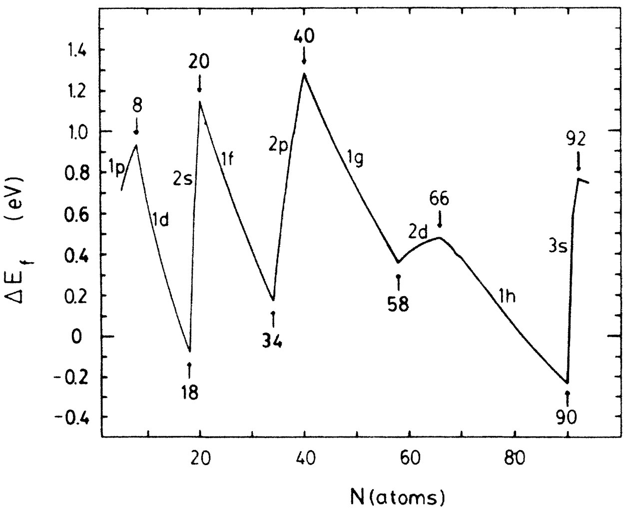

FIG. 1. Vacancy-formation energy as a function of cluster size. Each part of the curve is labeled by the external electronic shell of perfect clusters in that size range.

This alternate behavior is remarkable since it is different from the behavior shown by the cohesive energy. The cohesive energy $E_c(N)$ is defined

$$E_c(N)=E_{\text{at}}-E(N)/N \tag{3}$$

where $E_{\text{at}}=E(N=1)$ is the energy of the free atom, calculated in the same model (that is, a jellium cluster with only one atom). Figure 2 shows that $E_c(N)$ presents maxima or shoulders for N corresponding to filled electronic shells. This means that closed-shell clusters are comparatively stable with respect to clusters with adjacent sizes. The maxima of E_c occur for $N=8$, 20, 40, 58, and 92, which are the experimental magic numbers of Na clusters.[6,7] Shoulders appear for $N=18$ and 34, which are also magic numbers of secondary importance.[6,7] The absence of special features at the shell-closing numbers $N=68$ and 90, which will be explained below, agrees with the corresponding absence of special features in the experimental mass spectra.[6,7] The extrapolation of $E_c(N)$ to large N is consistent with the experimental bulk cohesive energy (1.11 eV).

The special stability of closed-shell clusters is clearly displayed by the second derivative of $E(N)$, that is, by the function $\Delta_2(N)=E(N+1)-2E(N)+E(N-1)$. It is well known[6,7] that this function has pronounced peaks for the shell-closing numbers $N=8$, 18, 20, 34, 40, 58, and 92, in the case of Na clusters. In contrast, Fig. 1 shows that only some of them have maximum stability against vacancy formation, i.e., those with $N=8$, 20, 40, and 92.

We also show in Fig. 2 the cohesive energy $E_c(N_v)$ of defect clusters, that is, clusters with a vacancy, defined as

$$E_c(N_v)=E_{\text{at}}-E(N_v)/N . \tag{4}$$

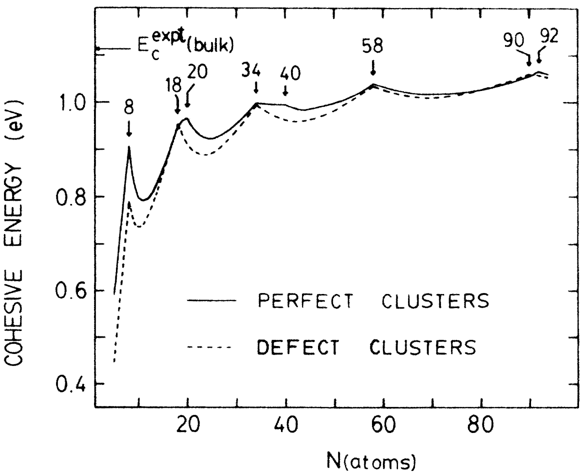

FIG. 2. Cohesive energy of perfect and defect clusters.

In this equation $E(N_v)$ indicates again the total energy of an N-atom cluster with a vacancy at its center. Notice from Eqs. (2)–(4) that

$$\Delta E_f(N) = -N[E_c(N_v) - E_c(N)] \ . \tag{5}$$

This is a useful relation for gaining insight into the behavior of $\Delta E_f(N)$.

In Fig. 2 we turn our attention to the numbers $N=20$, 40, and 92. $E_c(N)$ presents peaks at these numbers, but nothing like that occurs in the corresponding $E_c(N_v)$. This is due to the loss of cohesion after formation of the vacancy. The loss of cohesion at these particular sizes is larger than for neighbor sizes and accounts for the relative maxima in Fig. 1, that is, for the resistance to vacancy formation.

Although $\Delta E_f(N)$ has been obtained from total-energy self-consistent density-functional calculations, the features of Fig. 1 can be understood by looking at the evolution of the one-electron levels as the particle size increases. This behavior is shown in Fig. 3. Data is given for both perfect clusters and defect clusters.

First considering the perfect clusters, there is a big change in the total energy of the cluster when a shell becomes filled and occupation of the next level begins. This is due to the energy gap between the two levels and accounts for the magic-number effects. However, the $2d$ and $1h$ levels are so close in energy in the neighborhood of $N=68$ that the shell-closing effect is not important. This accounts for the absence of relevant features in $E_c(N)$ at $N=68$ (see Fig. 2). Furthermore, the similarity of the energy eigenvalues of the $1h$ and $3s$ levels near $N=90$ accounts for the absence of features in $E_c(N)$ at $N=90$.

Turning now to defect clusters we observe that most low-l orbitals (for instance $1s$, $2s$, or $2p$) rise in energy (that is they become less bound) and high-l orbitals lower their energies when a vacancy is formed. This is not surprising since the vacancy can be considered as a repulsive potential for electrons. Of course, this effect is more pronounced for low-orbital angular momentum, so the occupation of high-l orbitals becomes somehow favored.

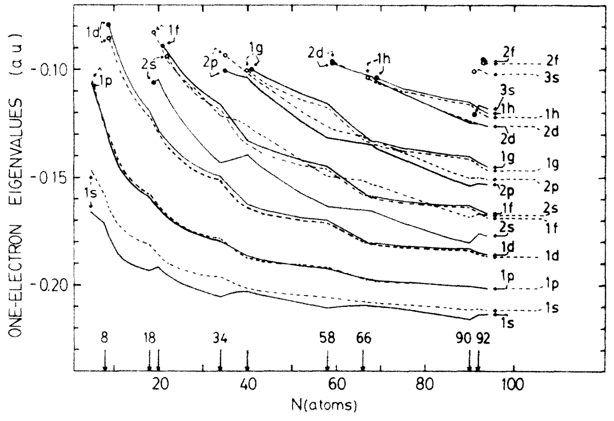

FIG. 3. Evolution of one-electron energy level eigenvalues with cluster size. Continuous and dashed lines indicate levels of perfect and defect clusters, respectively. The circles mark the first appearance of a given orbital in perfect and defect clusters. This occurs at the same value of N in some cases ($1d$, $2p$, $2d$, $3s$, $2f$) but not in others ($2s$, $1f$, $1g$, $1h$). Notice that, for any size N, only occupied levels are shown.

This effect has important consequences. A perfect cluster with $N=20$ has a closed-shell configuration $1s^2 1p^6 1d^{10} 2s^2$. In contrast, when a vacancy is formed, the electronic configuration becomes $1s^2 1p^6 1d^{10} 1f^2$, that is, an inversion of the order of the $2s$ and $1f$ levels has occurred. In other words, the cluster of 20 atoms with a vacancy is not a closed-shell cluster, which accounts for the loss of cohesion after formation of a vacancy at $N=20$. A similar argument applies to $N=40$. The perfect cluster of this size has an electronic configuration $1s^2 1p^6 1d^{10} 2s^2 1f^{14} 2p^6$. But by forming a vacancy the electronic configuration becomes $1s^2 1p^6 1d^{10} 2s^2 1f^{14} 2p^5 1g^1$, which is not a closed-shell configuration. In conclusion, the occupation of the $1f$ and $1g$ shells starts at smaller N for clusters with a vacancy, in comparison with perfect clusters. However, the shell-closing numbers $N=34$ and 58 are not affected since there is a further crossing in the filling order so that the $2s$ shell is completed before the $1f$ and also the $2p$ shell is completed before the $1g$. For this reason there is no substantial loss of cohesion when a vacancy is formed at $N=34$ and 58.

A consequence of the shift of energy level eigenvalues with vacancy formation is that, for cluster sizes such that a low-l external orbital is partially occupied, the vacancy-formation energy increases with N. The opposite occurs during the occupation of high-l orbitals. This accounts for the maxima in ΔE_f at $N=8$, 20, 40, (66), and 92, and the minima at $N=18$, 34, 58, and 90 in Fig. 1. (Notice that $1d$ is a high-angular-momentum level relative to $1p$ and $2s$, whereas $2d$ is of low-angular momentum relative to $1g$ and $1h$.)

It was pointed out above that the very similar energy of the $2d$ and $1h$ levels of the perfect clusters with $N \simeq 68$ accounts for the absence of a peak in E_c at $N=68$. When forming a vacancy the $1h$ level falls below the $2d$ for $N<72$. This effect is responsible for shifting the weak relative maximum from $N=68$ to $N=66$ in Fig. 1.

Since the formation of the vacancy perturbs mainly the region around the cluster center, one could search for a correlation between ΔE_f and $\rho(r=0)$. We have obtained that such a correlation exists for values of $N=18$–20 and $N=90$–92, that is, when an external s shell is involved. In contrast, no correlation is found for other cases.

Before proceeding further, a brief comment on the values of ΔE_f may be in order. Studies of the first ionization potential V_{ion} of alkaline clusters[5–6,12–15] show that the jellium model predicts the jumps of V_{ion} observed in the experiments.[16] However, the magnitude of the jumps is overestimated. We admit that a similar effect might occur in $\Delta E_f(N)$. This could account for the apparently large values of ΔE_f at the maxima in Fig. 1 and the rather low values at the minima (the theory predicts, in fact, a negative ΔE_f at $N=17, 18$ and $N=82$–90). The values of ΔE_f could be improved using a more refined model. However, such refined models are not easy to implement for large N. But from the success of the jellium model for alkali-metal clusters[5,6] we expect that the general features of Fig. 1 will still be valid in more refined models. The model used in this paper has been, in fact, successful in explaining the characteristic features of the mass distribution of mixed K_NMg clusters.[17] In this case, the positive background given in (1) is modified to account for the presence of the Mg atom at the cluster center. This was achieved by simulating the Mg^{2+} ion by a jellium of different (larger) density.

A question of interest is the extrapolation of ΔE_f to the limit $N=\infty$. Our results for $N<100$ show that we still are in a size region where quantum size effects dominate and that it is very difficult to extrapolate the results to the large N limit. However, an average value of ΔE_f is consistent with the experimental value for bulk sodium (0.42 eV).[18] In conclusion, the dominance of quantum size effects does not permit us to connect with the experimental work on small particles discussed by Morokhov and co-workers,[1,2] which pertains to larger particles.

Detailed, fine-structure features existing in the experimental mass spectra of alkaline clusters have been explained by Clemenger,[19] using a model of ellipsoidal distortions analogous to the shape variations among nuclei. For most sizes the predicted shape is ellipsoidal instead of spherical, so that the spherical shells are divided into ellipsoidal subshells. In Clemenger's model, clusters with $N=2$, 8, 20, 40, 58, and 92 remain spherical, but the rest become ellipsoidally deformed (in particular, $N=18$ and 34 become oblate ellipsoids).

The resistance of the magic clusters $N=8$, 20, 40, and 92 to ellipsoidal deformation correlates with their resistance to vacancy formation (maxima in Fig. 1), which is another kind of deformation. These clusters are thus strongly resistant against any kind of deformation. On the other hand, the ellipsoidal clusters of Clemenger's model have a lower ΔE_f (in the spherical model) than the spherical clusters. This is particularly noticeable around $N=18$, 34, and 90. In conclusion, one should contemplate the possibility that clusters with vacancies could be formed during the process of cluster growth in a supersonic expansion. This could provide a method of employing the extra energy of the hot clusters. This extra energy comes from the kinetic energy of incident atoms and from the gain in cohesive energy. Of course, formation of vacancies is less probable in the magic clusters. Finally, it is likely that our results might have implications for understanding the formation of mixed clusters.[8,20] In fact, our recent paper on K_NMg clusters[17] shows that the change in the K_N magic numbers due to Mg substitution can be understood in terms of the change of the one-electron levels induced by the attractive effect of the Mg ion.

ACKNOWLEDGMENT

This work was supported by La Comisión Asesora de Investigación Científica y Técnica (CAICyT), Grant No. 3265/83.

---

[1] I. D. Morokhov, S. P. Chizhik, N. T. Gladkik, L. K. Grigor'eva and S. V. Stepanova, Dokl. Akad. Nauk SSSR **247**, 1376 (1979) [Sov. Phys.—Dokl. **24**, 674 (1979)]; **248**, 603 (1979) [**24**, 769 (1979)]; Russ. Metall. **N5**, 172 (1979).

[2] I. D. Morokhov, V. I. Zubov, and V. B. Fedorov, Fiz. Tverd. Tela (Leningrad) **25**, 312 (1983) [Sov. Phys.—Solid State **25**, 178 (1983)].

[3] *The Inhomogeneous Electron Gas*, edited by S. Lundqvist and N. H. March (Plenum, New York, 1983); W. Kohn and L. J. Sham, Phys. Rev. **140**, A1133 (1965).

[4] M. Y. Chou, A. Cleland, and M. L. Cohen, Solid State Commun. **52**, 645 (1984).

[5] W. D. Knight, W. A. de Heer, W. A. Saunders, K. Clemenger, M. Y. Chou, and M. L. Cohen, Chem. Phys. Lett. **134**, 1 (1987).

[6] M. L. Cohen, M. Y. Chou, W. D. Knight, and W. A. de Heer, J. Phys. Chem. **91**, 3141 (1987).

[7] W. D. Knight, K. Clemenger, W. A. de Heer, W. A. Saunders, M. Y. Chou, and M. L. Cohen, Phys. Rev. Lett. **52**, 2141 (1984).

[8] M. M. Kappes, M. Schär, and E. Schumacher, J. Phys. Chem. **91**, 658 (1987).

[9] M. P. Iñiguez, J. A. Alonso, and L. C. Balbás, Solid State Commun. **57**, 85 (1986).

[10] M. P. Iñiguez, J. A. Alonso, M. A. Aller, and L. C. Balbás, Phys. Rev. B **34**, 2152 (1986).

[11] M. P. Iñiguez and J. A. Alonso, Z. Phys. D **2**, 177 (1986).

[12] W. Ekardt, Surf. Sci. **152**, 180 (1985).

[13] D. Beck, Solid State Commun. **49**, 381 (1984).

[14] W. D. Knight, W. A. de Heer, and W. A. Saunders, Z. Phys. D **3**, 109 (1986).

[15] M. Kappes, M. Schär, P. Radi, and E. Schumacher, J. Chem. Phys. **84**, 1863 (1986).

[16] W. A. Saunders, K. Clemenger, W. A. de Heer, and W. D. Knight, Phys. Rev. B **32**, 1366 (1985).

[17] C. Baladrón, J. A. Alonso, and M. P. Iñiguez, J. Phys. F **17**, L197 (1987).

[18] R. Feder and H. P. Charbnau, Phys. Rev. **149**, 464 (1966).

[19] K. Clemenger, Phys. Rev. B **32**, 1359 (1985).

[20] M. Kappes, P. Radi, M. Schär, and E. Schumacher, Chem. Phys. Lett. **119**, 11 (1985).